

## N-C Axially Chiral Anilines Electronic Effect on Barrier to Rotation and A Remote Proton Brake

Yumiko Iwasaki, Ryuichi Morisawa, Satoshi Yokojima, Hiroshi Hasegawa, Christian Roussel, Nicolas Vanthuyne, Elsa Caytan, Osamu Kitagawa

► **To cite this version:**

Yumiko Iwasaki, Ryuichi Morisawa, Satoshi Yokojima, Hiroshi Hasegawa, Christian Roussel, et al.. N-C Axially Chiral Anilines Electronic Effect on Barrier to Rotation and A Remote Proton Brake. Chemistry - A European Journal, Wiley-VCH Verlag, 2018, 24 (17), pp.4453-4458. 10.1002/chem.201706115 . hal-01771098

**HAL Id: hal-01771098**

**<https://hal-univ-rennes1.archives-ouvertes.fr/hal-01771098>**

Submitted on 7 Apr 2019

**HAL** is a multi-disciplinary open access archive for the deposit and dissemination of scientific research documents, whether they are published or not. The documents may come from teaching and research institutions in France or abroad, or from public or private research centers.

L'archive ouverte pluridisciplinaire **HAL**, est destinée au dépôt et à la diffusion de documents scientifiques de niveau recherche, publiés ou non, émanant des établissements d'enseignement et de recherche français ou étrangers, des laboratoires publics ou privés.

# N–C Axially Chiral Anilines: Electronic Effect on Barrier to Rotation and A Remote Proton Brake

Yumiko Iwasaki,<sup>[a]</sup> Ryuichi Morisawa,<sup>[a]</sup> Satoshi Yokojima,<sup>[b]</sup> Hiroshi Hasegawa,<sup>[b]</sup> Christian Roussel,<sup>[c]</sup> Nicolas Vanthuyne,<sup>[c]</sup> Elsa Caytan,<sup>[d]</sup> and Osamu Kitagawa<sup>\*[a]</sup>

**Abstract:** *N*-Aryl-*N*-methyl-2-*tert*-butyl-6-methylaniline derivatives exhibit a rotationally stable N–C axially chiral structure and the rotational barriers around an N–C chiral axis increased with the increase in electron-withdrawing character of *para*-substituent on the aryl group. X-ray crystal structural analysis and the DFT calculation suggested that the considerable change of the rotational barriers by the electron

effect of *para*-substituents is due to the disappearance of resonance stabilization energy caused by the twisting of *para*-substituted phenyl group in the transition state. This structural property of the N–C axially chiral anilines was employed to reveal a new acid-decelerated molecular rotor caused by the protonation at the remote position (remote proton brake).

## Introduction

Chiral compounds owing to rotational restriction around an N–C bond have received remarkable attention in the area of synthetic organic chemistry.<sup>[1]</sup> Syntheses of various N–C axially chiral compounds and their applications to asymmetric reactions have been investigated by many groups.<sup>[1–3]</sup>

Meanwhile, the application of N–C axially chiral compounds to molecular devices (molecular rotors) was recently reported.<sup>[4]</sup> Molecular rotors, which can control the rate of a bond rotation by external stimuli, are one of the most fascinating classes of molecular devices.<sup>[5]</sup> Shimizu and our groups found acid-accelerated molecular rotor based on the rotation around a N–C bond (Figure 1). Shimizu et al. revealed that N–C bond rotation of *N*-(quinolin-8-yl)succinimide **I** is significantly accelerated (the rotational barrier of **I** is significantly lowered) by the addition of protic acid.<sup>[4b]</sup> The acid-mediated significant acceleration is caused by the stabilization of the planar transition

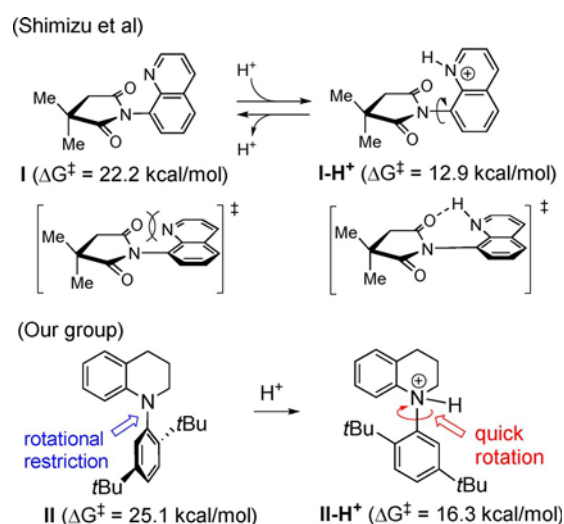


**Figure 1.** Acid-accelerated molecular rotors based on the rotation around N–C bond.

state by the formation of an intramolecular hydrogen bond (proton grease). In our molecular rotor (N–C axially chiral cyclic amine **II**), the addition of protic acid led to the remarkable acceleration of N–C bond rotation through change upon hybridization of nitrogen atom due to the formation of protonated amine **II-H<sup>+</sup>**.<sup>[4c]</sup> Acid-catalyzed acceleration of rotation about a N–C bond added a new facet to N–C axially chiral chemistry and further developments are expected.

We report herein the atropisomerism of new N–C axially chiral amines in the almost unexplored *N*-aryl-*N*-methyl-2-*tert*-butyl-6-methylaniline series. The considerable change of the rotational barriers according to the electronic effect of the *para*-substituent on the aryl group was supported by DFT calculation as well as X-ray crystal structural analysis (Figure 2), and this structural property was applied to the design of an

[a] Y. Iwasaki, R. Morisawa, Prof. O. Kitagawa  
Department of Applied Chemistry  
Shibaura Institute of Technology  
3-7-5 Toyosu, Kohto-ku, Tokyo, 135-8548 (Japan)  
E-mail: kitagawa@shibaura-it.ac.jp

[b] Prof. S. Yokojima, Dr. H. Hasegawa  
School of Pharmacy  
Tokyo University of Pharmacy and Life Sciences  
1432-1, Horinouchi, Hachioji, Tokyo, 192-0392 (Japan)

[c] Prof. C. Roussel, Dr. N. Vanthuyne  
Aix Marseille Univ, CNRS, Centrale Marseille  
iSm2, Marseille (France)

[d] Dr. E. Caytan  
Univ Rennes, CNRS, ISCR-UMR 6226  
35000 Rennes (France)

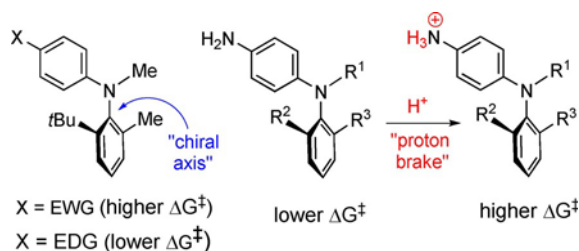


**Figure 2.** Considerable change of rotational barriers by the electronic effect in N–C axially chiral amines and the application to a remote proton brake.

unprecedented acid-decelerated molecular rotor caused by the protonation at remote position (remote proton brake, Figure 2).

## Results and Discussion

As mentioned above, although various N–C axially chiral compounds have been reported, almost all the compounds have amide or nitrogen-containing aromatic heterocyclic structures. Meanwhile, only a handful of reports on N–C axially chiral amines have been published.<sup>[4c,6]</sup> When we investigated the synthesis of rotationally stable N–C axially chiral amines (*N*-aryl-*N*-methyl-2-*tert*-butyl-6-methylaniline derivatives), a considerable change of the rotational barriers by *para*-substituents on aryl group was found. That is, *N*-(4-nitrophenyl)aniline **1a** has rotationally stable N–C axially chiral structure and the *ee* (99% *ee*) is almost unchanged on standing for 24 h at 50 °C in CCl<sub>4</sub>, while in *N*-(4-aminophenyl)aniline derivatives **1f** prepared via the hydrogenation of **1a**, the initial *ee* (98% *ee*) significantly decreased (12% *ee*) on standing for 6 h at 50 °C (Figure 3).

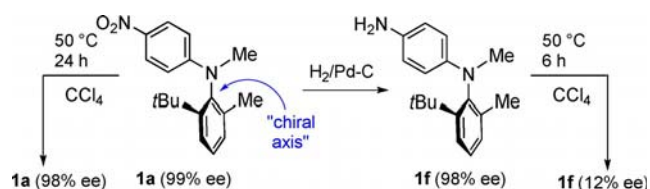
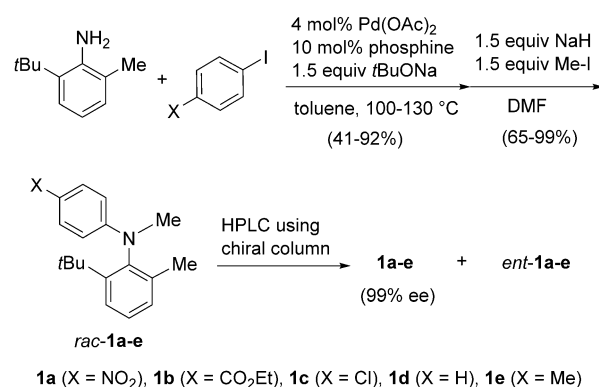


**Figure 3.** Rotationally stability of a chiral axis in N–C axially chiral anilines.

This result suggests that the rotational barrier around the N–C bond (the rate of N–C bond rotation) is significantly influenced by the electronic effect of remote *para*-substituent on aryl group. Quite recently, Clayden et al. reported the synthesis of a focused library of axially chiral *N*-aryl-2-*tert*-butyl-6-methylanilines (diaryl amines), their crystal structures and two examples of rotational barriers.<sup>[7]</sup> However, there is no mention on such electronic effect. To elucidate the relationship between the electronic effect and the rotational barriers, racemic *N*-aryl-*N*-methyl-2-*tert*-butyl-6-methylaniline derivatives *rac*-**1a–f** bearing various *para*-substituents (X = NO<sub>2</sub>, CO<sub>2</sub>Et, Cl, H, Me, NH<sub>2</sub>) on aryl group were prepared through Buchwald–Hartwig amination of 2-*tert*-butyl-6-methylaniline with *para*-substituted iodobenzene followed by N-methylation, and their enantiomers were separated by chiral HPLC method (Scheme 1).



**Scheme 1.** Synthesis of N–C axially chiral anilines **1a–f** bearing various *para*-substituents.

Subsequently the racemization rates of **1a–f** were measured in CCl<sub>4</sub> and their rotational barriers were evaluated through the Eyring relation (Table 1). It was found that the rotational barriers show decreasing tendency with increasing the electron-donating character of *para*-substituents X. The energy difference ( $\Delta\Delta G^\ddagger$ ) between *para*-nitro derivative **1a** possessing the highest rotational barrier ( $\Delta G^\ddagger = 29.4 \text{ kcal mol}^{-1}$ ) and *para*-amino derivative **1f** possessing the lowest rotational barrier ( $\Delta G^\ddagger = 24.8 \text{ kcal mol}^{-1}$ ) was  $4.6 \text{ kcal mol}^{-1}$  (Table 1).

**Table 1.** Rotational barriers of N–C axially chiral amines **1a–f** bearing various *para*-substituted phenyl groups.

Entry	X	<b>1</b>	$\Delta G^\ddagger_{\text{exp}}$ [kcal mol <sup>-1</sup> ] <sup>[a]</sup>	$t_{1/2, 298\text{K}}$ [days]	$\Delta G^\ddagger_{\text{calcd}}$ [kcal mol <sup>-1</sup> ] <sup>[b]</sup>
1	NO <sub>2</sub>	<b>1a</b>	29.4	2475	30.1
2	CO <sub>2</sub> Et	<b>1b</b>	28.2	304	29.1
3	Cl	<b>1c</b>	26.7	27.1	27.8
4	H	<b>1d</b>	26.5	19.0	27.5
5	Me	<b>1e</b>	26.1	9.2	26.9
6	NH <sub>2</sub>	<b>1f</b>	24.8	1.0	25.7

[a]  $\Delta G^\ddagger$  value at 298 K based on racemization experiment. [b]  $\Delta G^\ddagger$  value at 298 K based on DFT calculation (M06-2X/cc-pVTZ level) for the N–C bond rotation.

Furthermore, in the Hammett plot analysis, a relatively good linear relationship was observed between Hammett  $\sigma$ -values and the rotational barriers ( $R^2 = 0.97$ , Figure 4). Thus, the rotational barriers in N–C axially chiral amines **1a–f** were quantitatively related to the electronic character of *para*-substituent.

Kondo et al. have reported similar relationship between the electronic effect and rotational barriers in N–C axially chiral imides bearing various *para*-substituted benzoyl groups.<sup>[8]</sup>

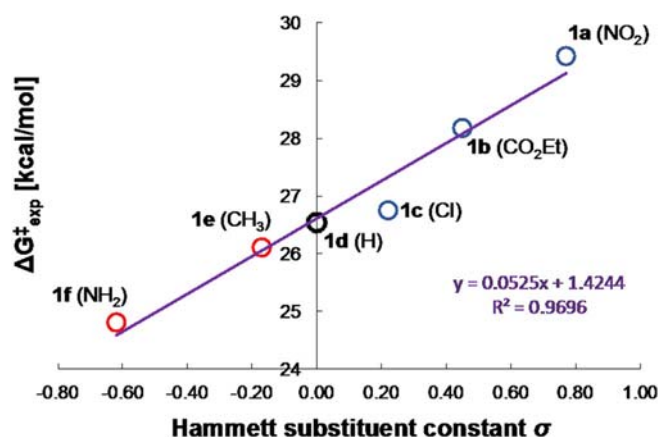


Figure 4. Hammett plot of the rotational barriers in anilines 1 a-f.

However, the *para*-substituents possessing negative resonance effect such as nitro and ester groups were not investigated, and the energy difference between *para*-CF<sub>3</sub> derivative possessing the highest rotational barrier and *para*-dimethylamino derivative possessing the lowest rotational barrier was slight ( $\Delta\Delta G^\ddagger = 1.4 \text{ kcal mol}^{-1}$ ) in comparison with that of our N-C axially chiral amines ( $\Delta\Delta G^\ddagger = 4.6 \text{ kcal mol}^{-1}$ ). In addition, although they postulated the transition state structure during the N-C bond rotation and used it to explain the change of  $\Delta G^\ddagger$  by the electronic effects, the analysis by computational method such as MO or DFT calculation was not conducted.

We attempted the elucidation of the relationship between the electronic effect and the rotational barriers in amines **1** by considering the transition state structure based on the DFT calculation as well as the X-ray crystal structural analysis. Initially, X-ray crystal structural analyses of *para*-nitro derivative **1a** possessing the highest rotational barrier and *para*-methyl derivative **1e** possessing the second lowest rotational barrier were conducted (Figure 5, *para*-amino derivative **1f** possessing the lowest rotational barrier was oil).<sup>[9]</sup> The crystal structures of **1a** and **1e** show that the *para*-substituted phenyl groups are perpendicular with the nitrogen plane ( $\angle \text{Me-N-C1'-C2'}$ : **1a** =  $-172.64^\circ$ , **1e** =  $-169.85^\circ$ ) while the 2-*tert*-butyl-6-methylphenyl groups are almost perpendicular to the nitrogen plane

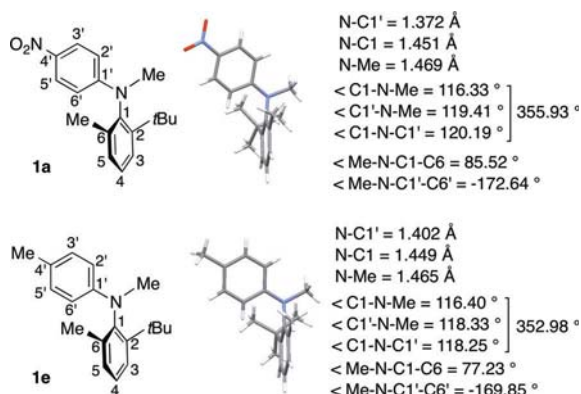


Figure 5. X-Ray crystal structures of **1a** and **1e**.

( $\angle \text{Me-N-C1-C6}$ : **1a** =  $85.52^\circ$ , **1e** =  $77.23^\circ$ ). Thus, a lone pair on the nitrogen in **1a** and **1e** should mainly interact with the *para*-substituted phenyl group but not with the 2-*tert*-butyl-6-methylphenyl group in the ground state. Indeed, the distances of N-C1' bond in **1a** and **1e** are significantly shorter than other two N-C bonds (N-C1 and N-Me bonds). Understandably, N-C1' bond in **1a** is shorter than that in **1e** because of the strong negative resonance effect associated to the *para*-nitro group.

The transition states during N-C bond rotation in **1a** and **1f** were subsequently estimated by DFT method (Figures 6 and 7). The rotational barriers of **1a** and **1f** calculated at M06-2X/

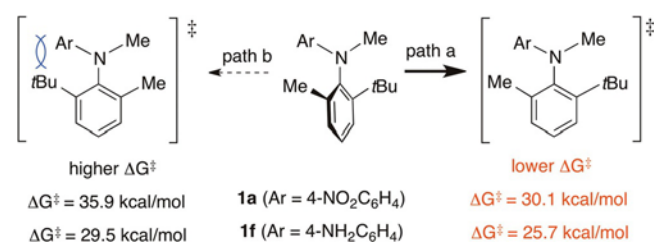
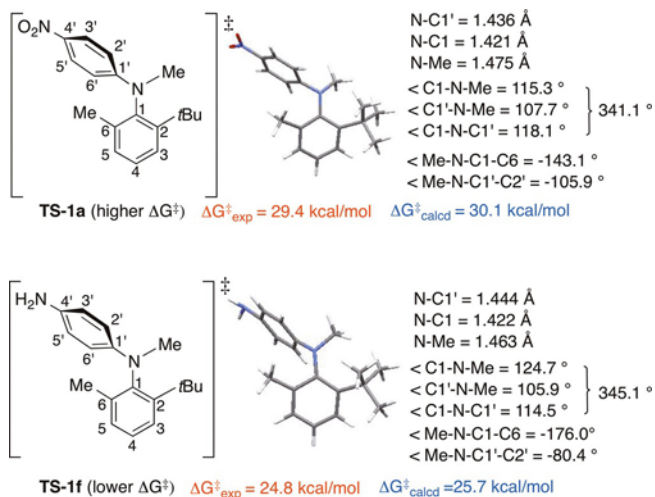


Figure 6. The rotational barriers of two possible rotation pathways evaluated by DFT calculation.

cc-pVTZ level corresponded reasonably well with the experimental  $\Delta G^\ddagger$  values (entries 1 and 6 in Table 1), and the transition state structures and the pathway during the N-C bond rotation provided beneficial information for elucidation of the electronic effect. Among two possible rotation pathways (paths a and b), path a which proceeds via the rotation of *ortho-tert*-butyl group toward *N*-methyl group side, is favored more than path b which occurs via the rotation of *ortho-tert*-butyl group toward *para*-substituted phenyl group (Figure 6, The rotational barriers via path a in **1a** and **1f** were 5.8 and 3.8 kcal mol<sup>-1</sup> lower than those via path b).

Interestingly, in the transition state structures **TS-1a** and **TS-1f** via path a, *para*-substituted phenyl groups are almost perpendicular to the nitrogen plane ( $\angle \text{Me-N-C1'-C2'}$ : **1a** =  $-105.9^\circ$ , **1f** =  $-80.4^\circ$ , Figure 7). The large twisting of *para*-substituted phenyl group may alleviate the steric repulsion with *ortho*-methyl group. Meanwhile, the twisting should cause the disappearance of the resonance stabilization which occurs in the ground state. The resonance stabilization energy in the ground state is linked to the magnitude of electron-withdrawing effect of *para*-substituent (X), and it follows that the loss of the stabilization energy by the twisting of *para*-substituted phenyl groups in the transition state increases with increasing the electron-withdrawing character of X. As a result, N-C axially chiral amines bearing stronger electron-withdrawing *para*-substituent possess higher rotational barrier.

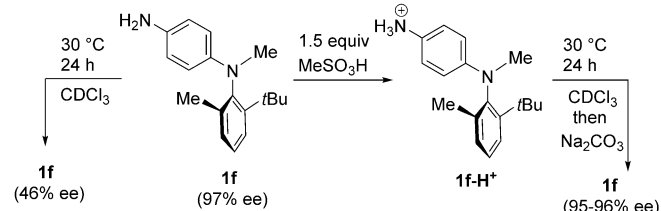
On the basis of the above results, we expected that the addition of protic acid to *para*-amino derivative **1f** may generate the *para*-ammonium derivative **1f-H<sup>+</sup>** to bring about a considerable increase in the rotational barriers due to the strong electron-withdrawing character of the ammonium group. In this case, the rotational barrier will be controlled by an exter-



**Figure 7.** The transition state structures during N–C bond rotation evaluated by DFT calculation and the origin of electronic effect.

nal factor but not by internal substituents such as **1 a–f**. In addition, in contrast to acid-accelerated molecular rotors (proton grease) shown in Figure 1, the protic acid will act as a remote brake during N–C bond rotation (proton brake).<sup>[10]</sup>

As already mentioned, the rotational barrier of **1 f** was not so high ( $\Delta G^\ddagger = 24.8 \text{ kcal mol}^{-1}$ ), and the initial *ee* (97% *ee*) of **1 f** lowered to 46% *ee* after standing for 24 h at 30 °C in  $\text{CCl}_4$  (Scheme 2). In contrast, in the presence of  $\text{MeSO}_3\text{H}$ , the de-



**Scheme 2.** The *ee* change of **1 f** in the presence or absence of  $\text{MeSO}_3\text{H}$ .

crease in the *ee* of **1 f** was slight (Scheme 2). That is, after standing  $\text{CCl}_4$  solution of **1 f** involving 1.5 equivalents of  $\text{MeSO}_3\text{H}$  for 24 h at 30 °C, the neutralization by aqueous  $\text{Na}_2\text{CO}_3$  solution and the extraction with ethyl acetate were conducted to recover **1 f** which presented 95–96% *ee* by chiral HPLC analysis (The slight decrease in the *ee* may be due to the N–C bond rotation of **1 f** but not **1 f-H<sup>+</sup>**).

Although we attempted to experimentally evaluate the rotational barrier of **1 f-H<sup>+</sup>**, it was difficult because the *ee* of **1 f** ( $24.8 \text{ kcal mol}^{-1}$ ) easily changed during the neutralization and the extraction process. Therefore, the rotational barrier of **1 f-H<sup>+</sup>** was evaluated by DFT method. The  $\Delta G^\ddagger$  value of **1 f-H<sup>+</sup>** ( $28.7 \text{ kcal mol}^{-1}$ ) calculated at M06-2X/6–311++G(d) level is similar to the experimental and calculated  $\Delta G^\ddagger$  values of *para*-ester derivative **1 b** ( $28.2$  and  $29.1 \text{ kcal mol}^{-1}$ ), and this value was 3.9 and  $3.0 \text{ kcal mol}^{-1}$  higher, respectively, in comparison with the experimental and the calculated values of **1 f**.

Variable temperature NMR (VT-NMR) is the method of choice to evaluate rotational barriers,<sup>[11]</sup> however this method could not be applied to **1 f-H<sup>+</sup>** which presents a too high a barrier and is not equipped with suitable diastereotopic protons. After a screening of several compounds, *N*-(4-aminophenyl)-*N*-propyl-2-isopropylaniline **2 f** was found to be an appropriate molecule for VT-NMR measurement.

In **2 f**, the selective protonation of *para*-amino group was also observed. When 0.32 equivalents of  $\text{MeSO}_3\text{H}$  was added to **2 f** in  $\text{CDCl}_3$ , a downfield shift of two aromatic hydrogens ( $\text{H}_a$ ) on *para*-aminophenyl group was noticed (Figure 8). The mag-

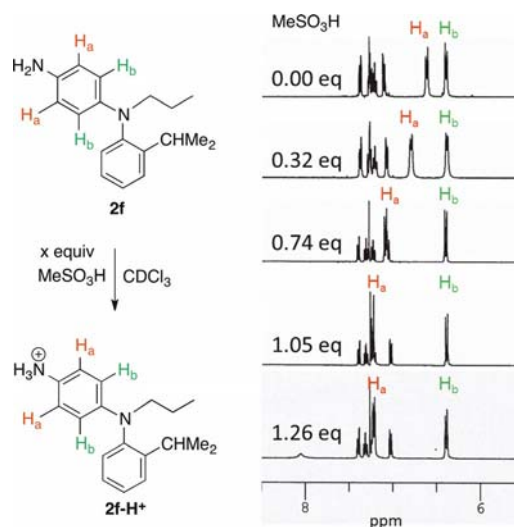


**Figure 8.**  $^1\text{H}$  NMR spectra of aromatic hydrogen of **2 f** in the presence or absence of  $\text{MeSO}_3\text{H}$  in  $\text{CDCl}_3$ .

nitude of the downfield shift is related to the amount of added  $\text{MeSO}_3\text{H}$  and reached a maximum limit by addition of 1.05 equivalents of  $\text{MeSO}_3\text{H}$ . In the proton addition, the chemical shift of the other two aromatic hydrogens ( $\text{H}_b$ ) was scarcely changed. Since the protonation at tertiary amino group is not preferred because of the severe steric hindrance, this result indicates that the protonation selectively occurs at  $\text{NH}_2$  group, and  $\text{H}_a$  and  $\text{H}_b$  being, respectively situated in *ortho*- and *meta*-position of the  $\text{NH}_2$  group.

VT-NMR experiment with **2 f** in  $[\text{D}_8]\text{toluene}$  was conducted in the presence or absence of  $\text{MeSO}_3\text{H}$ . The VT-NMR chart of two Me groups at isopropyl part are shown in Figure 9. In **2 f**, the two Me groups were completely equivalent and observed as a sharp signal bearing doublet coupling at ambient temperature (295 K). The broadening of a signal of the Me groups was observed around 220 K, and the signals of diastereotopic Me group due to an N–C axial chirality (slow rotation around an N–C bond) were formed around 175 K (left NMR spectra). In the presence of 1.5 equivalents of  $\text{MeSO}_3\text{H}$ , two Me groups of **2 f** showed a broad signal even at 315 K, and the formation of diastereotopic Me signals was observed around 260 K (right NMR spectra). Thus, the addition of  $\text{MeSO}_3\text{H}$  clearly reduced the rate of N–C bond rotation.

The rotational barriers of **2 f** and **2 f-H<sup>+</sup>** were evaluated by the line shape simulation using WinDNMR program.<sup>[11]</sup> The cal-

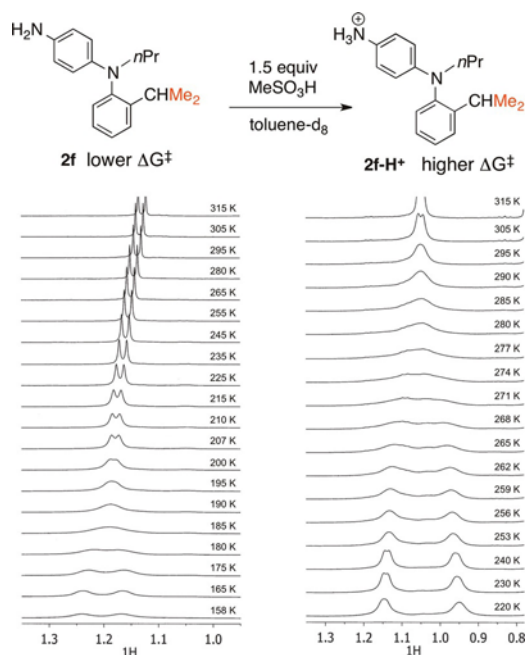


**Figure 9.** VT NMR spectra of isopropyl (dimethyl) group in **2f** and **2f-H<sup>+</sup>** in  $[D_8]$ toluene.

culated  $\Delta G^\ddagger$  values of **2f** and **2f-H<sup>+</sup>** were  $8.8 \pm 0.3 \text{ kcal mol}^{-1}$  at 175–185 K and  $12.8 \pm 0.3 \text{ kcal mol}^{-1}$  at 259–271 K, respectively. These results show that the addition of protic acid led to the brake of  $4 \text{ kcal mol}^{-1}$ , a value similar to that ( $3.9 \text{ kcal mol}^{-1}$ ) of proton brake in **1f** evaluated by DFT method.

## Conclusion

In conclusion, we found that *N*-aryl-*N*-methyl-2-*tert*-butyl-6-methylaniline derivatives have stable N–C axially chiral structure and their rotational barriers were considerably changed (controlled) by the *para*-substituent on aryl group. On the basis of X-ray crystal structural analysis and the DFT method, the considerable change of the rotational barriers by the electronic effect of *para*-substituents arose from resonance stabilization energy caused by the coplanarity of *para*-substituted phenyl group with the nitrogen plane in the ground state whereas that resonance stabilization energy was no more operating in the twisted transition state. Furthermore, the control of the rotational barrier through electronic factor was applied to design proton brake molecules in which the rotation rate around an N–C bond is decelerated by protonation at a remote position.

## Experimental Section

Melting points were uncorrected.  $^1\text{H}$  and  $^{13}\text{C}$  NMR spectra were recorded on a 400 MHz spectrometer. In  $^1\text{H}$  and  $^{13}\text{C}$  NMR spectra, chemical shifts were expressed in  $\delta$  (ppm) downfield from  $\text{CHCl}_3$  (7.26 ppm) and  $\text{CDCl}_3$  (77.0 ppm), respectively. HRMS were recorded on a double focusing magnetic sector mass spectrometer using electron impact ionization. Column chromatography was per-

formed on silica gel (75–150  $\mu\text{m}$ ). Medium-pressure liquid chromatography (MPLC) was performed on a  $25 \times 4 \text{ cm}$  i. d. prepacked column (silica gel, 10  $\mu\text{m}$ ) with a UV detector. High-performance liquid chromatography (HPLC) was performed on a  $25 \times 0.4 \text{ cm}$  i. d. chiral column with a UV detector.

### *N*-Methyl-*N*-(4-nitrophenyl)-2-*tert*-butyl-6-methylaniline (**1a**):

Under  $\text{N}_2$  atmosphere,  $\text{Pd}(\text{OAc})_2$  (18.0 mg, 0.080 mmol) and *rac*-BINAP (99.6 mg, 0.16 mmol) in toluene (1.5 mL) were stirred for 10 min at rt. 2-*Tert*-butyl-6-methylaniline (327 mg, 2.0 mmol) in toluene (1.5 mL), *t*BuONa (288 mg, 3.0 mmol) and 4-iodonitrobenzene (498 mg, 2.0 mmol) were added to the reaction mixture, and the mixture was stirred for 18 h at  $100^\circ\text{C}$ . The mixture was poured into saturated aqueous  $\text{NH}_4\text{Cl}$  solution and extracted with AcOEt. The AcOEt extracts were washed with brine, dried over  $\text{Na}_2\text{SO}_4$ , and evaporated to dryness. Purification of the residue by column chromatography (hexane/AcOEt = 10:1) gave *N*-(4-nitrophenyl)-2-*tert*-butyl-6-methylaniline (525 mg, 92%). Under  $\text{N}_2$  atmosphere, to NaH (60% assay, 80 mg, 2.0 mmol) in THF (6.0 mL) were added *N*-(4-nitrophenyl)-2-*tert*-butyl-6-methylaniline (286 mg, 1.0 mmol) and iodomethane (93  $\mu\text{L}$ , 1.5 mmol), and then the mixture was stirred for 45 min at RT and 2 h at  $50^\circ\text{C}$ . The mixture was poured into saturated aqueous  $\text{NH}_4\text{Cl}$  solution and extracted with AcOEt. The AcOEt extracts were washed with brine, dried over  $\text{Na}_2\text{SO}_4$ , and evaporated to dryness. Purification of the residue by column chromatography (hexane/AcOEt = 10) gave **1a** (295 mg, 99%). Enantiomers of **1a** were separated through MPLC using CHIRALPAK AY-H column [ $25 \times 1.0 \text{ cm}$  i.d.; 10% *i*PrOH in hexane; flow rate,  $2.0 \text{ mL min}^{-1}$ ; (+)-**1a**;  $t_{\text{R}} = 10.0 \text{ min}$ , (–)-**1a**;  $t_{\text{R}} = 22.5 \text{ min}$ ]. The *ee* of separated (+)-**1a** (less retained enantiomer) was determined by HPLC analysis using CHIRALPAK AS-H [ $25 \times 0.46 \text{ cm}$  i.d.; 15% *i*PrOH in hexane; flow rate,  $1.0 \text{ mL min}^{-1}$ ; (–)-**1a**;  $t_{\text{R}} = 6.3 \text{ min}$ , (+)-**1a**;  $t_{\text{R}} = 7.6 \text{ min}$ ]. **1a**: yellow solid; mp  $116\text{--}119^\circ\text{C}$  (racemic),  $116\text{--}119^\circ\text{C}$  [(+)-**1a**, 99% *ee*];  $[\alpha]_{\text{D}} = +34.6$  ( $c = 0.21$ ,  $\text{CHCl}_3$ , 99% *ee*); IR (neat)  $2955 \text{ cm}^{-1}$ ;  $^1\text{H}$  NMR ( $\text{CDCl}_3$ )  $\delta$ : 8.23 (1H, dd,  $J = 2.4, 8.8$ ), 7.92 (1H, dd,  $J = 2.8, 9.6 \text{ Hz}$ ), 7.45 (1H, dd,  $J = 1.6, 8.0 \text{ Hz}$ ), 7.26 (1H, t,  $J = 7.6 \text{ Hz}$ ), 7.19 (1H, dd,  $J = 1.2, 7.6 \text{ Hz}$ ), 6.71 (1H, dd,  $J = 2.8, 9.2 \text{ Hz}$ ), 5.98 (1H, dd,  $J = 2.8, 9.6 \text{ Hz}$ ), 3.27 (3H, s), 1.97 (3H, s), 1.28 (9H, s);  $^{13}\text{C}$  NMR ( $\text{CDCl}_3$ )  $\delta$ : 154.3, 148.1, 142.0, 137.9, 137.7, 130.2, 128.2, 127.1, 126.6, 125.4, 113.3, 109.0, 40.6, 35.9, 32.1, 18.2; MS ( $m/z$ ) 321 [ $M + \text{Na}^+$ ]; HRMS. Calcd for  $\text{C}_{18}\text{H}_{22}\text{N}_2\text{NaO}_2$  [ $M + \text{Na}^+$ ] 321.15790. Found: 321.15843.

### *N*-(4-Aminophenyl)-*N*-methyl-2-*tert*-butyl-6-methylaniline (**1f**):

10% Pd-C was added to (+)-**1a** (52.2 mg, 0.175 mmol) in EtOH (1.6 mL)-THF (0.4 mL) and the mixture was stirred for 1.5 h at  $0^\circ\text{C}$  under  $\text{H}_2$  atmosphere. AcOEt was added to the mixture and 10% Pd-C was removed by filtration. The filtrate was evaporated to dryness. Purification of the residue by column chromatography (hexane/AcOEt = 4:1) gave (+)-**1f** (37.8 mg, 80%). The *ee* of **1f** was determined by HPLC analysis using CHIRALCEL OD-3 [ $25 \times 0.46 \text{ cm}$  i.d.; 10% *i*PrOH in hexane; flow rate,  $1.0 \text{ mL min}^{-1}$ ; (+)-**1f**;  $t_{\text{R}} = 9.6 \text{ min}$ , (–)-**1f**;  $t_{\text{R}} = 10.8 \text{ min}$ ]. **1f**: dark brown oil;  $[\alpha]_{\text{D}} = +61.0$  ( $c = 0.26$ ,  $\text{CHCl}_3$ , 98% *ee*); IR (neat)  $2957 \text{ cm}^{-1}$ ;  $^1\text{H}$ -NMR ( $\text{CDCl}_3$ )  $\delta$ : 7.38 (1H, dd,  $J = 1.2, 7.6 \text{ Hz}$ ), 7.17 (1H, t,  $J = 7.6 \text{ Hz}$ ), 7.12 (1H, d,  $J = 6.4 \text{ Hz}$ ), 6.76 (1H, brs), 6.60 (1H, brs), 6.51 (1H, brs), 5.84 (1H, brs), 3.10 (3H, s), 1.94 (3H, s), 1.29 (9H, s);  $^{13}\text{C}$ -NMR ( $\text{CDCl}_3$ )  $\delta$ : 149.6, 144.8, 143.2, 139.8, 135.9, 130.0, 126.8, 126.0, 117.0, 116.6, 115.1, 110.6, 40.2, 35.7, 32.0, 18.5; MS ( $m/z$ ) 269 [ $M + \text{H}^+$ ]; HRMS. Calcd for  $\text{C}_{18}\text{H}_{25}\text{N}_2$  [ $M + \text{H}^+$ ] 269.20177. Found: 269.20173.

## Acknowledgements

This work was partly supported by JSPS KAKENHI (C17K08220).

- [1] For reviews, see: a) I. Takahashi, Y. Suzuki, O. Kitagawa, *Org. Prep. Proc. Int.* **2014**, *46*, 1; b) E. Kumarasamy, R. Raghunathan, M. P. Sibi, J. Sivaguru, *Chem. Rev.* **2015**, *115*, 11239.
- [2] Typical papers on syntheses of N–C axially chiral compounds: a) L. H. Bock, R. Adams, *J. Am. Chem. Soc.* **1931**, *53*, 374; b) C. Kashima, A. Katoh, *J. Chem. Soc. Perkin Trans. 1* **1980**, 1599; c) C. Roussel, M. Adjimi, A. Chemlal, A. Djafri, *J. Org. Chem.* **1988**, *53*, 5076; d) T. Kawamoto, M. Tomishima, F. Yoneda, J. Hayami, *Tetrahedron Lett.* **1992**, *33*, 3169; e) O. Kitagawa, M. Yoshikawa, H. Tanabe, T. Morita, M. Takahashi, Y. Dobashi, T. Taguchi, *J. Am. Chem. Soc.* **2006**, *128*, 12923; f) S. Brandes, M. Bella, A. Kjoersgaard, K. A. Jørgensen, *Angew. Chem. Int. Ed.* **2006**, *45*, 1147; *Angew. Chem.* **2006**, *118*, 1165; g) K. Tanaka, K. Takeishi, K. Noguchi, *J. Am. Chem. Soc.* **2006**, *128*, 4586; h) G. Bringmann, T. Gulder, B. Hertlein, Y. Hemberger, F. Meyer, *J. Am. Chem. Soc.* **2010**, *132*, 1151; i) S. Shirakawa, K. Liu, K. Maruoka, *J. Am. Chem. Soc.* **2012**, *134*, 916; j) K. Kamikawa, S. Arae, W.-Y. Wu, C. Nakamura, T. Takahashi, M. Ogasawara, *Chem. Eur. J.* **2015**, *21*, 4954; k) M. E. Diener, A. J. Metrano, S. Kusano, S. J. Miller, *J. Am. Chem. Soc.* **2015**, *137*, 12369; l) M. Hirai, S. Terada, H. Yoshida, K. Ebine, T. Hirata, O. Kitagawa, *Org. Lett.* **2016**, *18*, 5700.
- [3] Typical papers on synthetic application of N–C axially chiral compounds: a) D. P. Curran, H. Qi, S. J. Geib, N. C. DeMello, *J. Am. Chem. Soc.* **1994**, *116*, 3131; b) X. Dai, A. Wong, S. C. Virgil, *J. Org. Chem.* **1998**, *63*, 2597; c) O. Kitagawa, H. Izawa, K. Sato, A. Dobashi, T. Taguchi, M. Shiro, *J. Org. Chem.* **1998**, *63*, 2634; d) A. D. Hughes, D. A. Price, N. S. Simpkins, *J. Chem. Soc. Perkin Trans. 1* **1999**, 1295; e) T. Bach, J. Schröder, K. Harms, *Tetrahedron Lett.* **1999**, *40*, 9003; f) M. Sakamoto, M. Shigekura, A. Saito, T. Ohtake, T. Mino, T. Fujita, *Chem. Commun.* **2003**, 2218; g) J. Clayden, H. Turner, M. Helliwell, E. Moir, *J. Org. Chem.* **2008**, *73*, 4415; h) A. J. Ayitou, J. L. Jesuraj, N. Barooah, A. Ugrinov, J. Sivaguru, *J. Am. Chem. Soc.* **2009**, *131*, 11314; i) A. Nakazaki, K. Miyagawa, N. Miyata, T. Nishikawa, *Eur. J. Org. Chem.* **2015**, 4603; j) A. J. Clark, D. P. Curran, D. J. Fox, F. Ghelfi, C. S. Guy, B. Hay, N. James, J. M. Phillips, F. Roncaglia, P. B. Sellars, P. Wilson, H. Zhang, *J. Org. Chem.* **2016**, *81*, 5547; k) M. Matsuo-ka, M. Goto, A. Wzorek; V. A. Soloshonok, O. Kitagawa, *Org. Lett.* **2017**, *19*, 2650; V. A. Soloshonok, O. Kitagawa, *Org. Lett.* **2017**, *19*, 2650.
- [4] a) B. E. Dial, R. D. Rasberry, B. N. Bullock, M. D. Smith, P. J. Pellechia, S. Profeta Jr., K. D. Shimizu, *Org. Lett.* **2011**, *13*, 244; b) B. E. Dial, P. J. Pellechia, M. D. Smith, K. D. Shimizu, *J. Am. Chem. Soc.* **2012**, *134*, 3675; c) Y. Suzuki, M. Kageyama, R. Morisawa, Y. Dobashi, H. Hasegawa, S. Yokojima, O. Kitagawa, *Chem. Commun.* **2015**, *51*, 11229.
- [5] Typical papers on molecular rotors: a) H. Iwamura, K. Mislow, *Acc. Chem. Res.* **1988**, *21*, 175; b) T. R. Kelly, H. Silva, R. Silva, *Nature* **1999**, *401*, 150; c) N. Koumura, R. W. J. Zijlstra, R. A. van Delden, N. Harada, B. L. Feringa, *Nature* **1999**, *401*, 152; d) G. S. Kottas, L. I. Clarke, D. Horinek, J. Michl, *Chem. Rev.* **2005**, *105*, 1281; e) S. P. Fletcher, F. Dumur, M. M. Pollard, B. L. Feringa, *Science* **2005**, *310*, 80; f) A. Coskun, M. Banaszak, R. D. Asztumian, J. F. Stoddart, B. A. Grzybowski, *Chem. Soc. Rev.* **2012**, *41*, 19.
- [6] a) T. Mino, Y. Tanaka, T. Yabusaki, D. Okumura, M. Sakamoto, T. Fujita, *Tetrahedron: Asymmetry* **2003**, *14*, 2503; b) T. Kawabata, C. Jiang, K. Hayashi, K. Tsubaki, T. Yoshimura, S. Majumdar, T. Sasamori, N. Tokitoh, *J. Am. Chem. Soc.* **2009**, *131*, 54; c) K. Hayashi, N. Matubayashi, C. Jiang, T. Yoshimura, S. Majumdar, T. Sasamori, N. Tokitoh, T. Kawabata, *J. Org. Chem.* **2010**, *75*, 5031; d) T. Mino, M. Asakawa, Y. Shima, H. Yamada, F. Yagishita, M. Sakamoto, *Tetrahedron* **2015**, *71*, 5985.
- [7] R. Costil, H. J. A. Dale, N. Fey, G. Whitcombe, J. V. Matlock, J. Clayden, *Angew. Chem. Int. Ed.* **2017**, *56*, 12533. The synthetic method of N–C axially chiral diaryl amines by Clayden *et al* differs from our method.
- [8] a) K. Kondo, T. Iida, H. Fujita, T. Suzuki, R. Wakabayashi, K. Yamaguchi, Y. Murakami, *Tetrahedron* **2001**, *57*, 4115. In addition, in several aniline derivatives, the relationship between the rotational barriers around an N–Ar bond and the electronic effect have been investigated in detail, while these anilines are rotationally unstable or achiral. b) L. Lunazzi, C. Magagnoli, D. Macciantelli, *J. Chem. Soc. Perkin Trans. 2* **1980**, *0*, 1704; c) D. Casarini, E. Foresti, L. Lunazzi, D. Macciantelli, *J. Am. Chem. Soc.* **1988**, *110*, 4527; d) C. Boga, S. Cino, G. Micheletti, D. Padovan, L. Prati, A. Mazzanti, N. Zanna, *Org. Biomol. Chem.* **2016**, *14*, 7061.
- [9] CCDC 1558932 (**1a**) and 1558933 (**1e**), contain the supplementary crystallographic data for this paper. These data are provided free of charge by The Cambridge Crystallographic Data Centre.
- [10] Typical papers on molecular brake: a) T. R. Kelly, M. C. Bowyer, K. V. Bhas- kar, D. Bebbington, A. Garcia, F. Lang, M. H. Kim, M. P. Jette, *J. Am. Chem. Soc.* **1994**, *116*, 3657; b) M. Takeuchi, T. Imada, S. Shinkai, *Angew. Chem. Int. Ed.* **1998**, *37*, 2096; *Angew. Chem.* **1998**, *110*, 2242; c) P. Jog, R. Brown, D. Bates, *J. Org. Chem.* **2003**, *68*, 8240; d) L. E. Harrington, L. S. Cahill, M. J. McGlinchey, *Organometallics* **2004**, *23*, 2884; e) O. Hirata, M. Takeuchi, S. Shinkai, *Chem. Commun.* **2005**, 3805; f) J. Yang, Y. Huang, J. Ho, W. Sun, H. Huang, Y. Lin, H. Huang, S. Huang, H. Lu, I. Chao, *Org. Lett.* **2008**, *10*, 2279; g) K. Hirose, K. Ishibashi, H. Shiba, Y. Doi, Y. Tobe, *Chem. Eur. J.* **2008**, *14*, 5803.
- [11] a) C. Wolf, *Dynamic Stereochemistry of Chiral Compounds: Principles and Applications*, RSC Publishing: Cambridge, **2008**; b) D. Casarini, L. Lunazzi, *J. Org. Chem.* **1988**, *53*, 182; c) J. Clayden, S. P. Fletcher, J. J. W. McDouall, S. J. M. Rowbottom, *J. Am. Chem. Soc.* **2009**, *131*, 5331.